CHEMISTRY
A EUROPEAN JOURNAL

(Dimethylaminomethyl)trifluorosilane, $Me_2NCH_2SiF_3$—A Model for the α-Effect in Aminomethylsilanes

Norbert W. Mitzel,*[a] Krunoslav Vojinović,[a] Thomas Foerster,[b] Heather E. Robertson,[b] Konstantin B. Borisenko,[b] and David W. H. Rankin[b]

Dedicated to Professor Hans-Heinz Karsch on the occasion of his 60th birthday

Abstract: $F_3SiCH_2NMe_2$ was prepared as a model for the investigation of the nature of the α-effect in α-aminosilanes, by fluorination of $Cl_3SiCH_2NMe_2$ with SbF_3. Under less mild conditions Si–C bond cleavage was also observed, leading to the double adduct $F_4Si(Me_2NCH_2SiF_3)_2$, which was characterised by a crystal structure analysis showing that the central SiF_4 unit is connected to $Me_2NCH_2SiF_3$ via Si···N dative bonds and F···Si contacts. $F_3SiCH_2NMe_2$ was characterised by multinuclear NMR spectroscopy (^1H, ^{13}C, ^{15}N, ^{19}F and ^{29}Si), gas-phase IR spectroscopy and mass spectrometry. It is a dimer in the crystal (X-ray diffraction, crystal grown in situ), held together by two Si–N dative bonds. In solution and in the gas phase the compound is monomeric. The structure of the free molecule, determined by gas-phase electron diffraction, showed that, in contrast to former postulates, there are no attractive Si···N interactions. Ab initio calculations have been carried out to explain the nature of the bonding. $F_3SiCH_2NMe_2$ has an extremely flat bending potential for the Si-C-N angle; the high degree of charge transfer from the Si to the N atoms which occurs upon closing the Si-C-N angle is in the opposite direction to that expected for a dative bond. The topology of the electron density of $F_3SiCH_2NMe_2$ was analysed. Solvent simulation calculations have shown virtually no structural dependence on the medium surrounding the molecule. The earlier postulate of Si→N dative bonds in SiCN systems is discussed critically in light of the new results.

Keywords: α-effect · amines · electron diffraction · noncovalent interactions · silicon

Introduction

Organosilicon compounds that have a donor function in a position geminal to a silicon atom show unusual reactivities. Often these changes in reactivity have been attributed to an "α-effect",[1] but this term has also been used in other circumstances and might thus be misleading.

[a] Prof. Dr. N. W. Mitzel, Dr. K. Vojinović
Institut für Anorganische und Analytische Chemie, Westfälische Wilhelms-Universität Münster
Corrensstrasse 30, 48149 Münster (Germany)
Fax:(+49) 251-833-6007
E-mail: mitzel@uni-muenster.de

[b] T. Foerster, Dr. H. E. Robertson, Dr. K. B. Borisenko, Prof. D. W. H. Rankin
School of Chemistry, University of Edinburgh
West Mains Road, Edinburgh EH9 3JJ (UK)

Supporting information for this article is available on the WWW under http://www.chemeurj.org/ or from the author.

This reactivity enhancement has been used commercially for a number of (aminomethyl)alkoxysilanes and other α-functionalised alkoxycarbosilanes, which are used as polymer cross-linkers and as surface-modification and adhesion-mediating agents.[2] The hydrolysis of the alkoxy functions is strongly accelerated in these compounds in comparison with (aminoalkyl)alkoxysilanes, in which the amino functions are further from the silicon centres. This opens up the possibility of replacing methoxy groups by the less reactive ethoxy functions, which has the advantage that the much less toxic ethanol (instead of methanol) is released upon hydrolysis—an important improvement in application safety.

There are also reports on the facilitated Si–C bond cleavage by hydrolysis or alcoholysis[3] in compounds containing the SiCN unit, and on the use of α-aminosilanes as aminomethylating reagents for aldehydes, which is also based on the specific weakening of the Si–C bonds in SiCN units.[4]

Despite the wide applicability of α-aminosilanes, the development of such systems is still based on references to the

DOI: 10.1002/chem.200500359

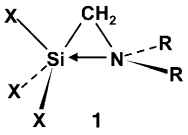

1

"α-effect" which involve the picture of a three-membered SiCN ring system **1**[5] stemming from the 1960s.

In the corresponding chemistry of boron, the existence of three-membered BCN rings **2** with dative B–N bonds is well established.[6] However, there is as yet no experimental proof of such a three-membered ring unit in SiCN systems, so the reasons for the "α-effect" remain vague and the nature of bonding in such systems is still debatable.

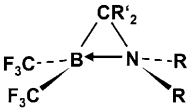

2

In recent years we have established that related systems containing SiNN (silylhydrazine) and SiON (hydroxylaminosilane) units can indeed form stable three-membered ring systems. The most intriguing examples are $ClH_2SiONMe_2$[7] and $F_3SiONMe_2$[8] for the SiON systems and $F_3SiN(SiMe_3)NMe_2$ and $F_3SiN(SnMe_3)NMe_2$ for the SiNN systems.[9]

Our investigations into the SiCN systems have so far been restricted to the parent systems $H_3SiCH_2NMe_2$[10] and $Cl_3SiCH_2NMe_2$,[11] but these compounds do not show significant attractive interactions between the Si and N atoms, which would lead to compression of the Si-C-N angle. However, some calculations on electronegatively substituted systems have predicted the compound $FH_2SiCH_2NMe_2$ to show deformation of this angle,[10] which could be the first proof of the existence of such an effect.

As the occurrence of SiON and SiNN three-membered ring systems could be proved unequivocally with the trifluorosilyl compounds $F_3SiONMe_2$ and $F_3SiN(SiMe_3)NMe_2$, we prepared $F_3SiCH_2NMe_2$ (**3**) as a simple model for the "α-effect" in aminomethylsilanes, and investigated its structure and the nature of its bonding. These studies, as well as the adduct formation of $F_3SiCH_2NMe_2$ with SiF_4, are reported below.

Results

Preparation and spectroscopic characterisation of $F_3SiCH_2NMe_2$: (Dimethylaminomethyl)trifluorosilane, $F_3SiCH_2NMe_2$ (**3**), was prepared by fluorination of the respective chlorosilane, $Cl_3SiCH_2NMe_2$,[11] with antimony trifluoride [Eq. (1)]. This reaction has to be conducted at low temperature to avoid Si–C bond cleavage and subsequently the formation of SiF_4. The fluorination is quite exothermic and the unexpected Si–C fluorination occurred with visible blackening of the reaction mixture. Simultaneous application of ultrasound and low temperatures was found to give the best yields. This kind of reactivity enhancement of the Si–C bond may also be promoted by the "α-effect".

$$Cl_3SiCH_2NMe_2 + SbF_3 \rightarrow SbCl_3 + F_3SiCH_2NMe_2\ (\mathbf{3}) \quad (1)$$

The identity of **3** was confirmed by NMR spectroscopy of the ^1H, ^{13}C, ^{15}N, ^{19}F and ^{29}Si nuclei, by gas-phase IR spectroscopy and by mass spectrometry. The ^1H and ^{13}C NMR spectra show the expected signals for the methylene and methyl groups. Interestingly, no $^2J_{F,C}$ coupling could be resolved for the signal of the methylene unit, which appears as three broad lines of a triplet due to the coupling to the adjacent hydrogen atoms.

The proton-decoupled ^{15}N NMR spectrum contains a single resonance at $\delta = -373.2$ ppm, which also does not show splitting due to coupling to the ^{19}F nuclei. This chemical shift does not indicate coordination of the nitrogen atom to an SiF_3 group in solution (compare: $H_3SiCH_2NMe_2$: $\delta(^{15}N) = -363.8$ ppm).[10] The ^{29}Si NMR spectrum shows a signal that is split into a quartet of triplets, due to the $^1J_{Si,F}$ coupling to the three fluorine atoms (236.9 Hz) and a $^2J_{Si,CH}$ coupling to the two protons of the methylene unit (4.6 Hz). The shift of $\delta = -65.6$ ppm could be regarded as typical for an alkyltrifluorosilane and is comparable with the chemical shift of F_3SiCH_2OMe at $\delta = -69.4$ ppm.[12] The typical shifts to low frequencies upon hypercoordination of the silicon atom, frequently found for other systems,[13] cannot be observed for **3** in solution, which indicates the presence of free molecules. The ^{19}F NMR data ($\delta = -61.9$ ppm) are also similar to those of F_3SiCH_2OMe ($\delta = -65.3$ ppm).[12] This interpretation is also consistent with the absence of splitting of the methylene signals at low temperatures which would be expected to occur upon ring formation due to the chemical inequivalence of equatorial and axial protons in puckered rings.

In those cases where Si–C bond cleavage occurs during the fluorination of $Cl_3SiCH_2NMe_2$ the resulting SiF_4 reacts as a Lewis acid, leading to complexation of the molecules of **3** through their N atoms [Eq. (2)].

$$SiF_4 + F_3SiCH_2NMe_2\ (\mathbf{3}) \rightarrow F_4Si(Me_2NCH_2SiF_3)_2\ (\mathbf{4}) \quad (2)$$

This complex **4** crystallises in large, well-formed crystals on the walls of the ampoule that contains the sample after separation of the volatile products from the remainder of the reaction mixture. The formation of **4** is reversible and **4** is stable only in the solid state (see below). It sublimes readily, which indicates cleavage into the three components. Neither in the gas phase (mass spectrometry, IR spectroscopy) nor in solution (NMR spectroscopy) is it possible to prove the occurrence of **4**, but its components are observed instead.

To obtain a more detailed view of the bonding situation in **3** we determined the structure of the compound in the solid state by X-ray crystallography and in the gas phase by electron diffraction, and performed quantum chemical calculations to complement the experimental data and to shed more light on the nature of bonding and the α-effect in SiCN systems.

Experimental structural studies on $F_3SiCH_2NMe_2$

Crystal structure: A single crystal of **3** (m.p. −39 °C) was grown in situ in a capillary on the diffractometer. The crys-

tal belongs to the triclinic system, space group $P\bar{1}$, with two independent molecules (**3a**, **3b**) in the asymmetric unit. The structure determination showed the compound to crystallise as dimers in which the silicon atom of each molecule is coordinated to the nitrogen atom of the other. There are two crystallographically independent, inversion-symmetric, six-membered $Si_2C_2N_2$ rings adopting chair conformations (Figure 1). The structures of the two dimers are very similar (see Table 1), so we discuss the structure of one molecule only.

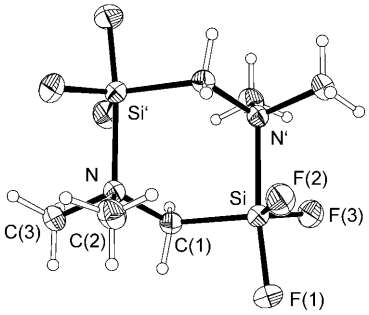

Figure 1. Crystal structure of $(F_3SiCH_2NMe_2)_2$. Only one of the two independent molecules in the asymmetric unit is shown.

Table 1. Bond lengths [Å] and angles [°] for $(F_3SiCH_2NMe_2)_2$ as determined by X-ray crystallography (XRD) and by ab initio calculations at the MP2/6-311G(d) level of theory.

Parameter	XRD		MP2/6-311 G(d)
	3a	**3b**	
Si–F(1)	1.641(1)	1.646(1)	1.641
Si–F(2)	1.605(1)	1.598(2)	1.629
Si–F(3)	1.601(1)	1.603(2)	1.624
Si–C(1)	1.898(2)	1.893(2)	1.902
Si–N′	2.070(2)	2.068(2)	2.128
N–C(1)	1.499(2)	1.502(2)	1.492
N–C(2)	1.492(2)	1.495(2)	1.485
N–C(3)	1.502(2)	1.503(2)	1.490
Si-C(1)-N	120.3(1)	120.5(1)	119.8
C(1)-Si-N′	92.6(1)	92.9(1)	91.1
F(1)-Si-F(2)	91.9(1)	92.3(1)	94.2
F(1)-Si-F(3)	92.6(1)	92.3(1)	94.6
F(2)-Si-F(3)	119.7(1)	119.8(1)	118.9
F(1)-Si-C(1)	94.2(1)	93.8(1)	94.7
F(2)-Si-C(1)	121.8(1)	117.9(1)	121.2
F(3)-Si-C(1)	117.8(1)	121.6(1)	118.1
F(1)-Si-N′	173.2(1)	173.4(1)	174.2
F(2)-Si-N′	84.4(1)	84.2(1)	82.6
F(3)-Si-N′	84.3(1)	84.6(1)	82.7
C(1)-N-C(2)	108.8(1)	109.0(1)	109.5
C(1)-N-C(3)	107.4(1)	106.8(1)	107.3
C(2)-N-C(3)	106.0(1)	106.0(1)	106.6
Si′-N-C(1)	111.6(1)	111.9(1)	112.3
Si′-N-C(2)	113.8(1)	113.6(1)	112.9
Si′-N-C(3)	108.9(1)	109.3(1)	108.0

The dative Si···N distances are 2.070(2) Å and are therefore within the established range for adducts of typical organotrifluorosilanes: 1-amino-8-trifluorosilylnaphthalene (2.318 Å),[14] 2,2,2-trifluorobenzo[*g*]-1λ^4,4,6-azadithia-2λ^5-silabicyclo[3.3.0]hexane (1.988 Å) and 2,2,2-trifluorobenzo[*g*]-1λ^4,4,6-azadithia-2λ^5-silabicyclo[3.3.0]hexane (1.965 Å)[15] as well as the dipyridine adduct of SiF_4 (1.932 Å)[16] and the 2,2′-bipyridine adduct of SiF_4 (1.981 and 1.972 Å).[17]

The coordination geometry at the silicon atoms is almost trigonal bipyramidal. The axial Si–F bond lengths (*trans* to the Si···N bonds) are 1.641(1) Å and are therefore longer than the equatorial Si–F bonds (1.601(2) and 1.603(2) Å). The F_{ax}-Si-F_{eq} angles are 91.9(1)° and 92.3(1)° and the F(1)-Si-C(1) angle is 94.2(1)°; that is, all are close to the ideal 90° for a trigonal bipyramid. Accordingly, the angles between the equatorial silicon substituents are close to 120°: F(2)-Si-F(3) 119.7(1)°, F(2)-Si-C(1) 121.8(1)° and F(3)-Si-C(1) 117.8(1)°. The Si–C (1.898(2) Å) and N–C (1.492(2) to 1.502(2) Å) distances are all longer than typical bonds of these types in the absence of hypercoordination.

Most intriguingly, the Si-C-N angle, which could be indicative of a direct attractive interaction between the Si and N atoms of one monomer molecule and thus prove the existence of the "α-effect" on a structural basis, is 120.3(2)° and thus much wider than expected even for a molecule without attractive Si···N forces, for which an angle close to the tetrahedral value could be expected. However, the hypercoordination at the silicon atoms and the dimerisation make it difficult to predict the amount of strain in this compound and the electronic effects on the bonding situation of the adjacent carbon atom and its valence angles. Comparison with the structural parameters of related compounds is helpful in this context. F_3SiCH_2OMe is monomeric in its crystals, and has a methylene group between a SiF_3 group and an electronegative unit. It has an Si-C-O angle of 107.1(1)°.[12] The aminomethylaluminium and -gallium compounds Me_2Al-CH_2NMe_2 and $Me_2GaCH_2NMe_2$, which contain the earth metal centres instead of the Lewis-acidic F_3Si group, also crystallise as dimers and also show extremely wide valence angles MCN (M = Al, 121.0(1)°; M = Ga, 119.7(2)°) at their methylene units.[18] The formal adduct of HF to **3** is the zwitterionic $F_4SiCH_2NHMe_2$, which like **3** was found to exhibit a large Si-C-N angle (118.5° and 119.2°).[19]

It is therefore likely that these wide Si-C-N angles in crystalline **3** are the result of the dimerisation and formation of four-coordinate nitrogen and five-coordinate silicon atoms rather than effects resulting from strain or packing forces. The existence of weak F···HC hydrogen bonds between the molecules was shown by short contacts for F···H(CH_2) at 2.479 Å and F···H(CH_3) at 2.503 Å (Figure 2), which is in the established range for F···H–C hydrogen bonds[20] and shorter than the sum of the van der Waals radii of F and H (2.55 Å).[21]

First attempts to perform calculations on the molecular structure of the dimer of **3** resulted in an extreme lengthening of the Si···N contacts during the optimisation procedure at the HF/6-31G* and up to the B3LYP/6-31G* level of theory, which made it impossible to locate a stable ground-state geometry on the potential hypersurface. Only a more rigorous treatment of electron correlation using MP2 meth-

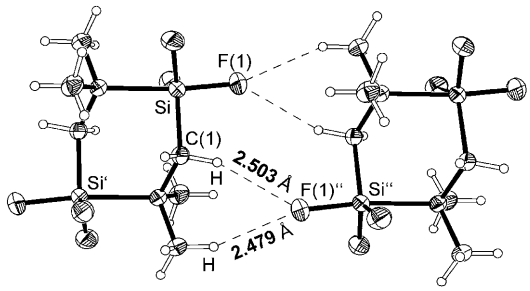

Figure 2. Weak C–H···F hydrogen bonds between two molecules of $(F_3SiCH_2NMe_2)_2$ in the crystal. The F···H distances between the other crystallographically independent dimeric molecules are F···H(CH_2) 2.499 Å and F···H(CH_3) 2.615 Å. The sum of the van der Waals radii of F and H is 2.55 Å.

ods and basis sets up to 6-311G* resulted in a stable and converging optimisation. The parameters describing this calculated geometry and the crystallographic data are summarised in Table 1 and show a reasonable but not very close agreement. Such phase-dependent differences in structures of typical Lewis base–acid adducts are now a well established and reasonably well understood phenomenon.[22]

Gas-phase structure: As the crystal structure results described above seem to be relevant only for the special conditions of the solid state, it was desirable to determine the structure of **3** in the gas phase, where it exists as a monomer. The results of an electron diffraction experiment are presented graphically in Figure 3, the structural parameters together with data from ab initio calculations [MP2/6-311++G(d,p)] in Table 2, and the experimental radial distribution and intensity curves in Figures 4 and 5.

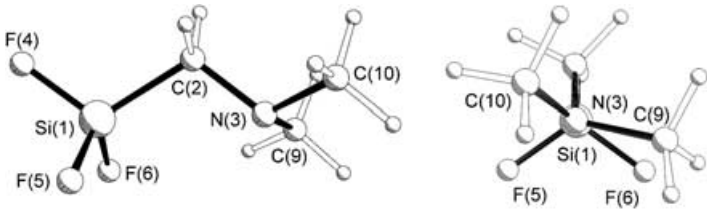

Figure 3. The gas-phase structure of monomeric $F_3SiCH_2NMe_2$ as obtained by electron diffraction. Right: a view along the Si–N vector, which shows that the molecule deviates markedly from C_S symmetry.

The $F_3SiCH_2NMe_2$ monomer (**3**) deviates substantially from the mirror symmetry that would be expected for the occurrence of an attractive Si···N interaction, as postulated for a molecule showing the classical "α-effect" and a three-membered SiCN ring with a dative Si···N bond. This distorted symmetry is indicated by the conformation of the molecule, in particular the Si-C-N-C torsion angles −149.1(17)° and 90.9(17)°, which describe the positions of the methyl groups. This is in good accord with theory. This asymmetric molecular geometry was also observed for gaseous $H_3SiCH_2NMe_2$,[10] which adopts an almost perfectly stag-

Table 2. Bond lengths r [Å] and bond ∢ and torsion angles τ [deg] for $F_3SiCH_2NMe_2$ (**3**) as determined by gas electron diffraction (GED) and by ab initio calculations.

Parameter	GED	MP2/6-311++G(d,p)
	r_a	r_e
r(Si(1)–F(4))	1.567(2)[a]	1.602
r(Si(1)–F(5))	1.567(2)[a]	1.596
r(Si(1)–F(6))	1.567(2)[a]	1.600
r(Si(1)–C(2))	1.854(5)	1.851
r(C(2)–N(3))	1.464(2)	1.467
r(N(3)–C(9))	1.456(2)[b]	1.460
r(N(3)–C(10))	1.456(2)[b]	1.460
r(CH)	1.115(10)	1.098[d]
∢(F(4)-Si(1)-C(2))	112.6(3)	110.6
∢(F(5)-Si(1)-C(2))	112.0(2)	111.1
∢(F(6)-Si(1)-C(2))	111.2(3)	113.7
∢(Si(1)-C(2)-H(7))	105.5(14)	105.2
∢(Si(1)-C(2)-H(8))	112.8(9)	112.6
∢(Si(1)-C(2)-N)	110.3(7)	110.8
∢(C(2)-N-C(9))	111.5(9)[c]	110.7
∢(C(2)-N-C(10))	111.5(9)[c]	110.7
∢(C(9)-N-C(10))	107.3(10)	109.9
τ(F(4)-Si(1)-C(2)-N(3))	−177.9(16)	−174.4
τ(Si(1)-C(2)-N-C(9))	90.9(17)	85.3
τ(Si(1)-C(2)-N-C(10))	−149.1(17)	−152.6

[a, b, c] The members of each group were assumed to be equal and were refined as a single parameter. [d] Average value.

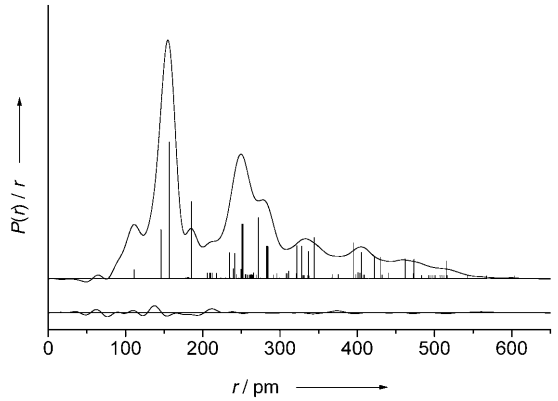

Figure 4. Radial distribution curve for $F_3SiCH_2NMe_2$ as obtained from a gas electron diffraction experiment.

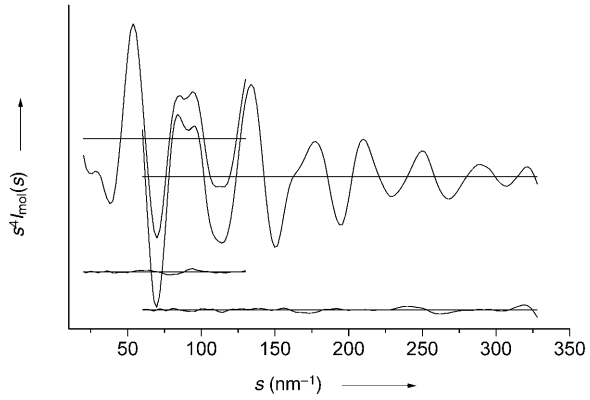

Figure 5. Molecular scattering intensity curves for $F_3SiCH_2NMe_2$ as obtained by gas electron diffraction.

gered conformation (τ(Si-C-N-C) 173.7(14)°, −62.4(12)°). Taking this into account, the conformation of **3** lies between the ideally staggered form adopted by $H_3SiCH_2NMe_2$ and that of a hypothetical C_S-symmetric $F_3SiCH_2NMe_2$ molecule, as expected for a structure dominated by attractive Si···N interactions. Although not very different, the Si-C-N angle in **3** (110.3(7)°) is 4° smaller than in $H_3SiCH_2NMe_2$ (114.7(3)°).

In comparison with the dimeric $(F_3SiCH_2NMe_2)_2$ (**3**) in the crystal, where the silicon atom is clearly five-coordinate, monomeric **3** has shorter Si–F distances (1.567(2) Å) and a shorter Si–C bond (1.854(5) Å) (solid dimer: 1.898(2) Å). The C–N distances also reflect a three-coordinate N atom in the gas phase (1.456(2)–1.464(2) Å), where they are shorter than in the solid state (1.492(2)–1.502(2) Å). The coordination geometry at silicon is an almost undistorted tetrahedron, as is best reflected by the three F-Si-C angles: 112.6(3)°, 112.0(2)° and 111.2(3)°.

Ab initio calculations on $F_3SiCH_2NMe_2$

Bending potentials: The structural studies did not provide evidence for the occurrence of a direct and pronounced attractive Si···N interaction in **3**. This contradicts the expectations from earlier reports on geminal systems with SiCN units, which led to the postulate of SiCN three-membered ring systems with Si···N donor–acceptor bonds nor are the structural results in accordance with those for related compounds with Si-N-N and Si-O-N units, in which pronounced attractive forces have been found to exist between the geminal nitrogen atoms and the silicon atoms of the highly electrophilic SiF_3 groups.[8,9]

We carried out bending potential calculations to find out how much energy is needed to distort the linking unit between the silicon and geminal nitrogen centres (the carbon atom of the CH_2 group in the case of $F_3SiCH_2NMe_2$) from its coordination geometry, which is assumed to be close to tetrahedral in the absence of attractive Si···N interactions. The calculations were performed on the basis of geometries fully optimised at the MP2/6-311G(d,p) level of theory with fixed Si-C-N angles. (Some of the calculations were also performed at the MP2/6-311++G(3df,2pd) level, but did not give significantly different results.) The resulting bending potential is shown in Figure 6.

The geometry of $F_3SiCH_2NMe_2$ (**3**) has C_1 symmetry at large Si-C-N angles, as was also shown in the gas-phase experiments. With a decrease in the Si-C-N angle this geometry comes closer to C_S symmetry and finally converges to a C_S structure at an angle of about 94°. In this C_S-symmetric structure the lone pair of electrons lies in the same plane as the SiCN unit, as would be required for an optimal N→Si dative interaction as postulated in the model of the α-effect. For comparison we have also calculated the potential curve for **3** ($F_3SiCH_2NMe_2$) fully restricted to C_S symmetry, which coincides with the C_1 curve below 94°, but shows a minimum at 102°, with a higher energy than the ground state.

Both are very flat potential curves; that of the C_1 structure is flatter on the low-angle side of the minimum than on the high-angle side, which is a rather uncommon feature. For comparison we have calculated the curve for the analogous compound $F_3CCH_2NMe_2$, which cannot show a geminal C···N interaction. (The ground state of $F_3CCH_2NMe_2$ has C_1 symmetry and a C-C-N angle of 112.0°.) This curve (Figure 6) is much steeper than those of the silicon compound and also steeper on the low-angle side, as expected for such a bending potential.

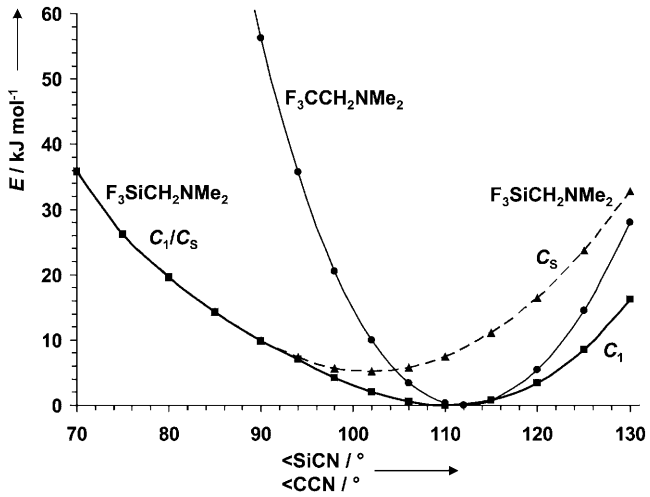

Figure 6. Bending potential curves for $F_3SiCH_2NMe_2$ (**3**): (■ for the geometrically unrestricted optimisations, ▲ for those restricted to C_S symmetry) and $F_3CCH_2NMe_2$ (●) as a function of the valence angle at the methylene bridge, as calculated at the MP2/6-311G(d,p) level of theory.

Atomic charges: The above results for $F_3SiCH_2NMe_2$ (**3**) indicate that there must be a contribution to the bonding that makes the methylene unit more easily deformable if a silicon atom is bonded to it than when it is bonded to carbon. Some information on the electronic behaviour can be obtained by observing the partial atomic charges of the Si, C and N atoms in **3** in its ground state and in the structure with the Si-C-N angle fixed at 70°, and by comparison with F_3SiCH_3 and NMe_3. These charges (see Table 3) were calculated by integration of the calculated electron density [MP2/6-311G(d,p)] of the atomic regions defined by the AIM (Atoms in Molecules) theory. The Si and N charges differ only slightly between the ground state and the structure with the artificially compressed Si-C-N angle (70°), but the positive charge on Si and the negative one on N are increased upon closing the Si-C-N angle, the opposite behav-

Table 3. Atomic charges as determined by integration over the calculated electron density [MP2/6-311G(d,p)] of the atomic regions defined by the AIM theory of the Si, C and N atoms in $F_3SiCH_2NMe_2$ (**3**) (ground state and structure with Si-C-N angle fixed at 70°) and of F_3SiCH_3 and NMe_3 for comparison.

Charge at	$F_3SiCH_2NMe_2$ (**3**)		F_3SiCH_3	NMe_3
	minimum	70°		
Si	+3.17	+3.20	+3.18	–
C	−0.27	−0.32	−0.69	+0.51
N	−0.80	−0.96	–	0.83

iour to that expected for an N→Si donor interaction suggested by the old α-effect postulate. The charge on the Si atom in both structures of **3** is also similar to that of F_3SiCH_3, a related compound without a geminal donor atom.

There is, however, a substantial difference between the charges on the N atoms in the two structures of **3**. Whereas the ground state of **3** has a charge on N that is very similar to that of NMe_3, the structure with the Si-C-N angle compressed to 70° has a negative charge 17% higher than in the ground state. This increase in negative charge on N is also responsible for the large increase in the molecular dipole moment with decreasing Si-C-N angle.

Very different, but as expected due to the difference in the electronic natures of the directly bonded atoms, are the charges on the silicon-bonded carbon atoms, which are much less negative in both structures of **3** than in F_3SiCH_3. This leads to a different polarity of the Si–C bond and could thus be one of the reasons for the difference in the reactive behaviour of "normal silanes" and "α-silanes".

To follow the changes in the charges more closely during contraction of the Si-C-N angle of **3**, we calculated the dependence of the atomic charges on this parameter, but used for this purpose the Mulliken charges from the calculations that were used to derive the bending potential. These are less costly to obtain but in absolute terms less reliable than the AIM charges mentioned above, although there have been reports about the limited reliability of AIM charges too;[23] Charges derived from the NBO calculations (see below) represent the same trend. As there is a problem of atomic charge definition, absolute values should be interpreted with care. The trends we discuss here are a more reliable basis for chemical interpretation.

For comparison we also calculated the trend of atomic charges for $F_3CCH_2NMe_2$ (the carbon analogue) depending on the corresponding C-C-N angle. These results are plotted in Figure 7 for the nitrogen atoms in $F_3SiCH_3NMe_2$ (**3**) and $F_3CCH_2NMe_2$, and in Figure 8 for the geminal silicon and carbon atoms, respectively.

Both figures show that with decreasing Si-C-N and C-C-N angles in $F_3SiCH_2NMe_2$ and $F_3CCH_2NMe_2$, respectively, there is a significant charge transfer from the fluorinated silicon/carbon atom to the nitrogen centre. However, the charge transfer for **3** is much greater—about twice as great—as for the carbon analogue. The large charge separation in **3** must be the basis for a pronounced electrostatic interaction between the silicon and nitrogen centres, which helps to stabilise the structures with low Si-C-N angles energetically. Thus this effect contributes to the flat bending potential of **3** and also leads to the build-up of a very pronounced molecular dipole moment in this silicon compound.

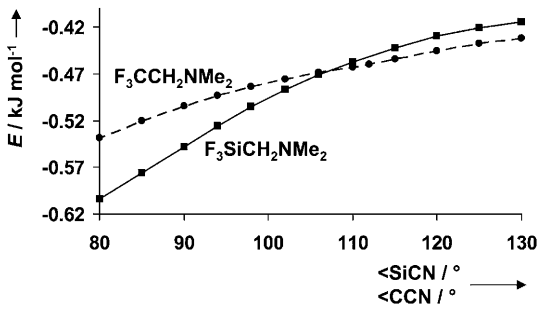

Figure 7. Atomic charges on the N atoms in $F_3SiCH_2NMe_2$ (**3**) (■) and $F_3CCH_2NMe_2$ (●) as functions of the valence angles at the methylene bridges, as calculated at MP2/6-311G(d,p) level.

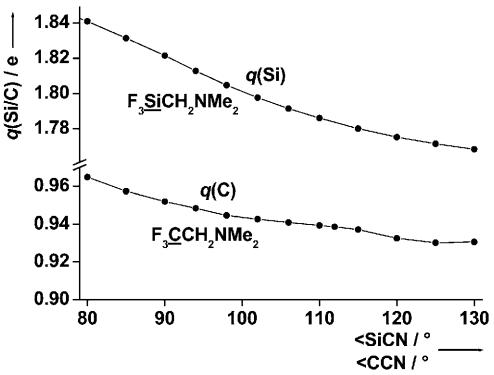

Figure 8. Atomic charges of the Si and C atoms in the F_3Si and F_3C groups of $F_3SiCH_2NMe_2$ (**3**) and $F_3CCH_2NMe_2$, respectively, as functions of the valence angles at the methylene bridges, as calculated at the MP2/6-311G(d,p) level of theory.

NBO calculations: To examine orbital interactions, which could help to determine the presence or absence of bonding interactions between the silicon and nitrogen atoms, we performed natural bond orbital (NBO) calculations.[24] Second-order perturbation theory analysis of the Fock matrix in the NBO basis was performed for the ground state of **3**, a structure with the Si-C-N angle fixed at 90° and one with a fixed angle of 70°, all at the MP2/6-311G(d,p) level of theory.

There are many smaller interactions of the negative hyperconjugation type, which contribute to the stabilisation of the structures. In the ground state ($\measuredangle$(Si-C-N) = 110.3°) we find the major interactions between lone pairs of electrons and acceptor *anti*-bonding orbitals in the following combinations: the lp(N)→σ*(CH) interactions with CH bonds of the methylene unit and both methyl groups (40 kJ mol^{-1}) and the lp(F)→σ*(SiF) interactions (up to 44 kJ mol^{-1}).

When the Si-C-N angle is closed to 90° the lone pair of electrons on nitrogen interacts less strongly with the σ*(CH) orbitals of the methylene unit, as the geometry approaches C_S symmetry, which reduces the respective overlap. The interaction with the σ*(CH) orbitals of the methyl groups is slightly increased and a weak lp(N)→σ*(SiF) interaction becomes visible (27 kJ mol^{-1}). In addition there are still larger interactions of the lp(F)→σ*(SiF) type (up to 52 kJ mol^{-1}).

Further closing of the Si-C-N angle to 80° increases the trend described above and in particular strengthens the lp(N)→σ*(SiF) interactions (62 kJ mol^{-1} for the interaction with the σ*(SiF) of the *anti* F atom, and 31 kJ mol^{-1} to each of the other σ*(SiF) orbitals).

The most extreme situation under investigation was a structure with a fixed Si-C-N angle of 70°. The NBO formalism already describes the Si···N interaction in this hypothetical molecule as an Si–N bond, but with a very polar electron distribution, made up from 6% of a formal $sp^{6.0}d^{4.1}$ hybrid at silicon and 94% of a formal $sp^{4.4}$ hybrid at nitrogen. For comparison, the Si–F bonds are described also as very polar bonds, with the *anti* Si–F bond being the most polar, made up from 10% of an $sp^{2.1}d^{1.5}$ hybrid at Si and 90% of an $sp^{1.3}$ hybrid at F, whereas the other two Si–F bonds are composed of 11% of an $sp^{3.0}d^{0.6}$ hybrid at Si and 89% of an $sp^{1.4}$ hybrid at F.

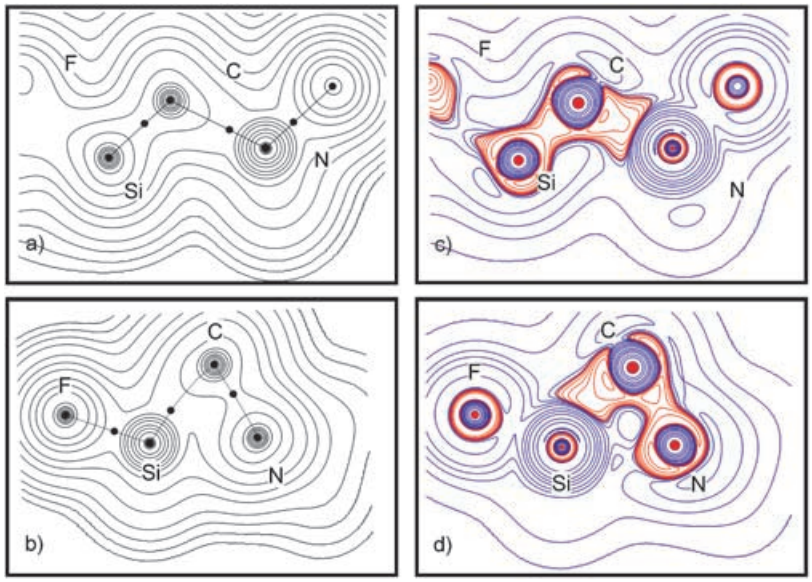

Figure 9. Topological analysis of the electron density in the SiCN plane of $F_3SiCNMe_2$. Electron densities including bond-critical points are shown for a) the ground state (∢(Si-C-N) = 110.3°); b) the structure with a fixed Si-C-N angle of 70° (contours are at values of 0.002×10^n e Å^{-1}, n = 0, 1, 2, 3···). The Laplacian function of the electron density is shown for c) the ground state as $-\nabla^2\rho(r)$ (∢(Si-C-N) = 110.3°) d) the structure with a fixed Si-C-N angle of 70° (contours are at values of 0.005×10^n, 0.01×10^n, 0.02×10^n e Å^{-5}, n = 0, 1, 2, 3···; positive values are in blue and negative values are in red).

Further stabilisation of this structure is achieved by donation of the electrons of this Si–N bond to σ*(SiF) orbitals (66 kJ mol^{-1} for the σ*(SiF) of the *anti* F atom and twice 41 kJ mol^{-1} for the interaction with the σ*(SiF) orbitals of the *gauche* F atoms]. Another large contribution towards the delocalisation of electrons is the interaction between the fluorine lone pairs and the σ*(SiN) orbitals (177 kJ mol^{-1} for the lp(F_{anti})→σ*(SiN) interaction and 86 kJ mol^{-1} for the lp(F_{gauche})→σ*(SiN) interaction). These interactions lead to weakening of a possible Si–N bond. In addition, interactions of the lp(F_{anti})→σ*(SiF) type are present with a contribution comparable with those for the cases described above.

The electron delocalisation stabilisation energies provided do not have any real physical meaning, but are helpful in assessing the relative strengths of orbital interactions in terms of the NBO picture.

Topologies of the electron densities: We have calculated the electron density maps of **3** at the MP2/6-311G(d,p) level for both the ground state and the structure with the Si-C-N angle fixed at 70°. The results of the analyses of the topologies of the electron densities[25] and the Laplace functions of these density maps for the plane containing the atoms Si, C and N are depicted graphically in Figure 9.

In density maps a and c we could not locate any bond-critical points between the Si and N atoms or ring-critical points in the SiCN three-membered ring system. This was expected for the ground state, but for the structure with the Si-C-N angle fixed at 70°, where the NBO analysis had already described the Si···N interaction as a very polar bond, this seemed surprising. The absence of an accumulation of electron density between the Si and N atoms and the absence of bond- and ring-critical points indicate that there is no significant covalent contribution in this interaction. However, care should be taken not to attribute too much importance to the presence or absence of bond-critical points for the existence or non-existence of a chemical bond.[26]

The Laplacians of the electron densities shown in Figures 9b and d are the appropriate tools for localising and characterising regions of local charge concentration or depletion. The local charge concentrations in the structures in Figure 9 help to visualise the positions of the lone pairs of electrons at the nitrogen atoms. These seem to be where expected for the ground state, but in the structure with the Si-C-N angle fixed at 70° (Si···N distance only 1.969 Å) the lone pair is bent towards the silicon atom.

In Table 4 values characterising the topologies of the electron density in these two states of $F_3SiCH_2NMe_2$ are compared with those in methyltrifluorosilane and trimethylamine, which serve as references for an alkyltrifluorosilane without a geminal donor nitrogen and a trialkylamine without a silicon atom geminal to nitrogen. It has recently been shown that theoretical and experimental electron density topologies of hypercoordinate silicon species show some systematic differences in the characteristic values of the electron densities $\rho(r_{BCP})$ and the values of the Laplacians $\nabla^2\rho(r_{BCP})$ at the bond-critical points (BCPs), but they follow the same trends.[27]

In general, shared interactions (covalent bonds) are characterised by relatively high electron densities $\rho(r_{BCP})$ and negative values of the Laplacians $\nabla^2\rho(r_{BCP})$, because charge is concentrated in the bonding regions. In contrast, closed-shell interactions (ionic bonds) have comparatively low ρ-

Table 4. Topology of the bonds in $F_3SiCH_2NMe_2$ (**3**) in the ground state, in the structure with the Si-C-N angle fixed at 70° and in the molecules $MeSiF_3$ and NMe_3 for comparison.

A–B	r(A–BCP)[a] [Å]	r(BCP–B)[a] [Å]	$\rho(r_{BCP})$[b] [e Å^{-3}]	$\nabla^2\rho(r_{BCP})$[c] [e Å^{-5}]
$F_3SiCH_2NMe_2$ (**3**) ground state ($\sphericalangle$(Si-C-N) = 110.3°):				
Si–C	0.702	1.147	0.898	6.707
Si–F(4)	0.668	0.929	0.875	26.184
Si–F(5)	0.666	0.926	0.888	26.709
Si–F(6)	0.668	0.928	0.878	26.297
C–N	0.609	0.859	1.772	−15.903
N–C(9)	0.876	0.583	1.802	−17.493
N–C(10)	0.879	0.581	1.794	−17.346
$F_3SiCH_2NMe_2$ (**3**) with <SiCN fixed to 70°:				
Si–C	0.712	1.162	0.803	7.368
Si–F(4)$_{anti}$	0.674	0.944	0.841	23.784
Si–F(5/6)	0.672	0.939	0.848	24.557
C–N	0.638	0.908	1.477	−9.695
N–C(9/10)	0.899	0.567	1.735	−16.328
$MeSiF_3$:				
Si–C	0.700	1.130	0.905	7.248
Si–F	0.668	0.931	0.873	25.941
NMe_3:				
N–C	0.859	0.574	1.832	−17.775

[a] Distances from the bond-critical points (BCPs) to the nuclear positions. [b] Electron density at the BCP. [c] Laplacian at the BCP.

(r_{BCP}) values and positive $\nabla^2\rho(r_{BCP})$ values at the BCPs, due to charge depletion and concentration of charge close to the nuclear positions.[28]

Comparison of the electron densities at the BCPs of the Si–F and Si–C bonds in $F_3SiCH_2NMe_2$ (**3**) (ground state) and F_3SiCH_3 shows only marginal differences. As expected, the Si–F bonds are characterised by a highly ionic contribution. For any hypercoordinate silicon atom one would have expected a decrease in these $\rho(r_{BCP})$ values for both Si–F and Si–C bonds. However, even where the Si-C-N angle is artificially forced to be 70°, there is only a small decrease in the electron densities at the BCPs.

Compared with the Si–C bonds in F_3SiCH_3, the electron density at the BCP in **3** is slightly lower and the Laplacian less positive. The C–N bond to the methylene group in **3** has a markedly higher electron density at the BCP than the N–C bonds to the methyl groups in this molecule or in NMe_3. The Laplacian of this bond in **3** is less negative. Although there are these small differences between the values of $\rho(r_{BCP})$ or $\nabla^2\rho(r_{BCP})$ in the ground state of **3** and the structure with the Si-C-N angle fixed at 70°, they are not sufficient to be comparable with hypercoordinate silicon compounds—proof again that the early α-effect postulate of a N→Si dative bond in SiCN units was incorrect.

Solvent model simulations: Solvent model simulations, which have recently been reported for an isoelectronic compound, $F_3SiONMe_2$, indicated that the central Si-O-N angle becomes smaller as the dielectric constant of the solvent increases.[9] This phenomenon was therefore investigated with respect to the Si-C-N angle in **3**, using self-consistent isodensity polarized continuum model (SCIPCM) calculations and geometry optimisations. Interactions between the molecule and the solvents benzene, acetone and water were assessed in terms of the resulting geometry of $F_3SiCH_2NMe_2$. The calculations were performed at the Hartree–Fock (HF) and hybrid DFT (B3LYP) levels of theory employing Pople's 6-31G* basis set in Gaussian 03 on the Columbus server cluster of the Rutherford Appleton Laboratories (UK).

Comparison of gas-phase ab initio parameters with those obtained from SCIPCM calculations reveals that no significant changes occurred to the geometry of **3**. However, small changes are to be expected as a consequence of solute–solvent interactions (Table 5). The parameter values indicate that they are stable not only across different geometry optimisation techniques but also across different levels of theory and basis sets (Tables 5 and 6). Therefore it seems reasonable to conclude that the Si-C-N angle is little affected by the solvent, in contrast to the situation for the isoelectronic $F_3SiONMe_2$.

Table 5. Selected parameters of ab initio and SCIPCM geometry optimisations at the HF/6-31G* level.

Parameter	Ab initio calculation	SCIPCM calculations		
		water	acetone	benzene
r(Si(1)–C(2)) [Å]	1.861	1.858	1.858	1.860
$\sphericalangle$(Si(1)-C(2)-N) [°]	113.1	113.0	112.8	112.9

Table 6. Selected parameters of ab initio and SCIPCM geometry optimisations at the B3LYP/6-311++G** level (for the free molecule) and B3LYP/6-31G* level (for the solvent simulations).

Parameter	Ab initio calculation	SCIPCM calculations		
		water	acetone	benzene
r(Si(1)–C(2)) [Å]	1.860	1.861	1.862	1.863
$\sphericalangle$(Si(1)-C(2)-N) [°]	112.8	112.6	112.7	113.1

The absence of a significant solvent effect—that is, interaction of the molecule with the polar surroundings through its molecular dipole moment—is demonstrated impressively by the solvent model calculations. This is surprising at first glance as the total molecular dipole moment obtained from the NBO calculations increases dramatically with decreasing Si-C-N angle (3.55 D for the ground state with $\sphericalangle$(Si-C-N) = 110.3° and 6.02 D for the structure with $\sphericalangle$(Si-C-N) = 70°). The dipole moment also changes the orientation when the Si-C-N angle is closed (see Figure 10).

As the angle deformation energies are comparatively small, one would have expected the energy gain from the dipole interactions with the solvent to overcompensate for the energy needed for an angle contraction. As it is well established that typical dative bonds are sensitive to the polar-

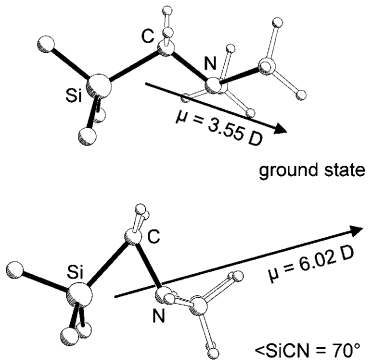

Figure 10. Orientations of the molecular dipole moments for the ground-state structure and that with the SiCN angle fixed at 70° as derived from calculations at the MP2/6-311G(d,p) level of theory.

ity and/or polarisability of the surrounding medium,[22] this is a further indicator of the absence of a N→Si dative bond contribution in $F_3SiCH_2NMe_2$ (**3**).

Crystal structure of $[F_4Si(F_3SiCH_2NMe_2)_2]$: As mentioned in the Experimental Section, the double adduct of $F_3SiCH_2NMe_2$ to SiF_4, $[F_4Si(F_3SiCH_2NMe_2)_2]$, was obtained as a crystalline material of which the structure (Figure 11) could be determined by single-crystal X-ray crystallography; structural data are listed in Table 7.

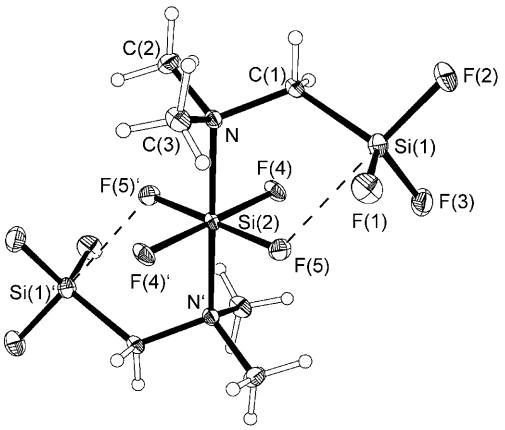

Figure 11. Crystal structure of $[F_4Si(F_3SiCH_2NMe_2)_2]$.

The adduct $[F_4Si(F_3SiCH_2NMe_2)_2]$ forms a centrosymmetric structure with a planar SiF_4 unit coordinated twice by the nitrogen atoms of the $F_3SiCH_2NMe_2$ components, with Si–N dative bonds exactly 2.000(1) Å long. Each of the fluorine atoms F(5) and F(5)′ of the SiF_4 unit forms a dative contact with a silicon atom of an $F_3SiCH_2NMe_2$ component, so that these are bonded twice to the SiF_4 unit. These contacts lead to marked distortion of the coordination geometry of the silicon atoms Si(1) and Si(1)′, which is between tetrahedral and trigonal bipyramidal, where the additional Si···F contact makes up one of the axial bonds (∢F(5)-Si(1)-F(2) = 178.6(1)°).

Table 7. Bond lengths [Å], bond angles [°] and torsion angles [°] for $[F_4Si(F_3SiCH_2NMe_2)_2]$.

Bond lengths:		Bond angles:	
Si(1)–F(3)	1.571(1)	N-C(1)-Si(1)	121.1(1)
Si(1)–F(1)	1.572(1)	F(1)-Si(1)-F(2)	102.6(1)
Si(1)–F(2)	1.589(1)	F(1)-Si(1)-F(3)	109.3(1)
Si(1)–C(1)	1.855(1)	F(2)-Si(1)-F(3)	102.8(1)
C(1)–N	1.501(1)	F(1)-Si(1)-C(1)	117.3(1)
N–C(2)	1.495(1)	F(2)-Si(1)-C(1)	102.7(1)
N–C(3)	1.499(1)	F(3)-Si(1)-C(1)	119.3(1)
N–Si(2)	2.000(1)	C(1)-N-C(2)	106.6(1)
Si(2)–F(4′)	1.648(1)	C(1)-N-C(3)	107.9(1)
Si(2)–F(5)	1.666(1)	C(2)-N-C(3)	107.1(1)
Si(1)···F(5)	2.489(1)	C(1)-N-Si(2)	111.0(1)
Si(1)″···F(4)	3.290(1)	C(2)-N-Si(2)	112.4(1)
		C(3)-N-Si(2)	111.8(1)
Torsion angles:		F(4)-Si(2)-F(5)	89.9(1)
C(1)-N-Si(2)-F(4)	141.4(1)	F(4)-Si(2)-F(5′)	90.1(1)
C(1)-N-Si(2)-F(5)	51.5(1)	F(4)-Si(2)-N	91.2(3)
		F(5)-Si(2)-N	86.7(3)
		F(4)-Si(2)-N′	88.8(3)
		F(5)-Si(2)-N′	93.3(3)
		F(5)-Si(1)-F(1)	77.3(1)
		F(5)-Si(1)-F(2)	178.6(1)
		F(5)-Si(1)-F(3)	76.0(1)
		F(5)-Si(1)-C(1)	76.0(1)

Like the free $F_3SiCH_2NMe_2$ (**3**) molecules, these units in the adduct have staggered conformations. However, they have an Si-C-N angle of 121.1(1)°, which is more than 10° wider than that in the free molecule. According to Figure 6 this requires only about 4 kJ mol^{-1} of deformation energy, which is more than compensated for by the formation of the new Si–N and Si···F bonds. This angle is also remarkably similar to that in dimeric $(F_3SiCH_2NMe_2)_2$ observed in the solid state (118.5°), and that in the zwitterionic compound $F_4SiCH_2NHMe_2$ (119.2°),[19] and suggests that this magnitude of the angle is an inherent property of an SiCN unit coordinated via both the Si and N atoms.

Conclusion

(Dimethylaminomethyl)trifluorosilane, $F_3SiCH_2NMe_2$ (**3**), is a simple model for an α-functional silicon compound for the study of an α-effect, which was postulated to be based on direct dative bonding between the Lewis-basic nitrogen centre and the Lewis-acidic silicon atom. The highly electrophilic character of the SiF_3 group should show the absence or presence of such an effect clearly.

Our studies show **3** to be dimeric in the solid state and monomeric in solution or in the gas phase. Experimental and theoretical studies show the ground state of the monomer to adopt an Si-C-N angle that gives no indication of a pronounced attractive Si···N interaction. It is therefore clear that **3** behaves in a very different way from the isoelectronic $F_3SiONMe_2$ (and related trifluorosilylhydrazines), for which the formation of three-membered SiON and SiNN rings has been found not only in the gas phase but also in the solid state. As **3** does not saturate the demand for electron densi-

ty at the trifluorosilyl group intramolecularly, it is by the formation of intermolecular dative bonds that it can stabilise itself in the solid state.

There is, however, a big difference between **3** and compounds without acceptor functions, as was shown by a parallel theoretical study of $F_3CCH_2NMe_2$. The silicon compound has a much flatter bending potential at the methylene group than the analogous carbon compound. Only 30 kJ mol^{-1} are necessary for an angle contraction of 30° relative to the ground state, whereas the carbon analogue requires more than 130 kJ mol^{-1} for the same contraction.

In classical donor–acceptor adducts electron density is transferred from the donor to the acceptor, although the amounts transferred might be quite small, as for instance in the case of the $H_3N\rightarrow SiF_4$ adduct, where a charge of only 0.08 e is shifted from the NH_3 unit to the SiF_4 unit.[29] However, in **3** this effect would be reversed. When the Si···N distance is decreased, electron density is transferred from silicon to nitrogen, which increases the charge separation already present due to the difference in electronegativities. This leads to an enormous increase in the molecular dipole moment.

The solvent model calculations (SCIPCM) delivered additional evidence that $F_3SiONMe_2$[9] and **3** exhibit different levels of intramolecular Si···N interactions. The calculations showed that the Si-C-N angle in **3**, in contrast to the Si-O-N angle in $F_3SiONMe_2$, is not much affected by the presence of solvents with widely varying dielectric constants. This suggests that the Si-C-N angle is hardly liable to change, except where strong intermolecular forces such as crystal packing exert their influence on the molecular structure, as the crystallographic data have shown for the solid-state structure of **3** presented here. This might also be the reason why $F_3SiONMe_2$ is stabilised in the polar solid state in the form of three-membered ring molecules, while the absence of this stabilisation for **3** leads to the dimerisation observed in the crystals.

The major difference between compounds containing SiCN units and their CCN analogues is the easy deformability of the methylene group in the SiCN unit. This, the high negative charge on the nitrogen atom and the unusual charge transfer could be seen as the major reasons for an observable effect in terms of the reactivity of the Si–C bond and the substitution reactions at the silicon atom, due to the increased nucleophilicity. In essence there is, however, no evidence for the existence of a classical dative N···Si bond between the geminal N and Si atoms. The classical picture of the α-effect in aminomethylsilanes involving such a dative bond is clearly misleading, and should not be used for further development of applications of substances containing these units.

The new results suggest several ways in which the effect might be increased, and which might therefore be helpful for a more rational development of new, more reactive α-silanes in the fields of application mentioned in the Introduction. Highly electronegative groups on silicon that are incapable of backbonding to silicon, such as perfluoroalkyl or perfluoroaryl groups, should be good candidates for enhancing the reactivity of Si functional groups. The use of highly polar solvents or highly polar groups within the molecules seems not to lead to observable differences in the molecular structure or charge distribution. However, interaction of donor solvents with the silicon atoms, leading to five-coordinate intermediates, is a possible way to increase reactivity towards nucleophilic substitution. The geminal nitrogen atom could assist in attracting donor solvents such as water or alcohols so that they are stabilised through hydrogen bonds and therefore placed in close proximity to the silicon centre. Even if the solvent–silicon interaction were weak, the chelating effect would increase the interaction strength.

On the theoretical side, we find it is necessary to predict a full reaction pathway for a nucleophilic substitution reaction at silicon with and without a geminal donor atom, to explore the empirically observed differences. The electronic effects in the SiCN unit can be monitored during such reactions. This work is in progress and will give more detailed insights into the details of the α-effect.

Experimental Section

Preparation: *N,N*-Dimethylaminomethyltrichlorosilane[11] (4.6 g, 24 mmol) was condensed onto a frozen (−196 °C) suspension of antimony trifluoride (4.5 g, 25 mmol) in toluene (15 mL). The mixture was allowed to warm very slowly to ambient temperature, with a cold bath as heat reservoir. All volatile components were removed in vacuo and collected in a cold trap. The contents of this trap were fractionated through a series of cold traps held at −50 °C, −60 °C, −78 °C and −196 °C. The product was collected in the −78 °C trap in the form of colourless crystals, which melt at −39 °C to give a slightly thermolabile colourless liquid that is best kept at liquid nitrogen temperature. The product yield was 24 % (0.8 g, 5.5 mmol). Application of ultrasound after melting of the mixture leads to better yields of up to 55 %. ^{1}H NMR (C_6D_6): δ = 1.79 (s, 2H, H_2C), 1.96 (s, 6H, H_3C); ^{13}C NMR: δ = 40.9 (t, $^1J_{C,H}$ = 122.4 Hz, CH_2), 48.5 ppm (q q, $^1J_{C,H}$ = 133.2 Hz, $^3J_{CN,CH}$ = 5.1 Hz, CH_3); ^{15}N{^{1}H} NMR: δ = −373.2 ppm (s); ^{19}F NMR: δ = −61.9 ppm (s); ^{29}Si NMR: δ = −65.6 ppm (q t, $^1J_{Si,F}$ = 236.9 Hz, $^2J_{Si,CH}$ = 4.6 Hz); IR (gas): $\tilde{\nu}$ = 2988 (m), 2963 (m), 2915 (w), 2882 (w), 2836 (m), 2784 (s, CH), 1464 (m), 1410 (w), 1314 (w), 1259 (m), 1161 (m), 1134 (w), 1100 (w), 1030 (s, SiF), 972 (vs), 891 (vs), 835 cm^{-1} (w); MS (EI, 70 eV): *m/z*: 143 ([*M*]$^+$), 126 ([M^+-CH_3]), 114 ([M^+-2CH_3]), 85 ([F_3Si]$^+$).

Crystal structures: A single crystal of $(F_3SiCH_2NMe_2)_2$ was generated by slowly cooling the melt after establishing a solid–liquid equilibrium, using a sample in a sealed Duran capillary. All but one of the crystals (an optically selected very small seed crystal) were then melted by locally warming the sample. Data collection was undertaken with a Nonius Turbo CAD4 diffractometer. Graphite-monochromated $Mo_{K\alpha}$ radiation was used (λ = 0.71073 Å). A crystal of $[F_4Si(F_3SiCH_2NMe_2)_2]$ was grown by sublimation and very quickly transferred in a drop of perfluoropolyether onto the tip of a glass fibre on the goniometer head of a Nonius Turbo CAD4 diffractometer. The structures were solved by direct methods and refined with the full-matrix least-squares procedure (SHELXTL[30]) against F^2. The plots of the molecular structures represent thermal ellipsoids at the 50 % probability level. Details of the crystal data and refinements are provided in Table 8. CCDC-267373 and CCDC-267374 contain the supplementary crystallographic data for this paper. These data can be obtained free of charge from the Cambridge Crystallographic Data Centre via www.ccdc.cam.ac.uk/data_request/cif.

Gas-phase structure determination: Electron diffraction data were collected on Kodak Electron Image photographic films using the Edinburgh

Table 8. Single-crystal X-ray diffraction experimental data.

	$F_3SiCH_2NMe_2$	$F_4Si(F_3SiCH_2NMe_2)_2$
formula	$C_3H_8F_3NSi$	$C_6H_{16}F_{10}NSi_3$
M_r	143.19	195.24
crystal system	triclinic	monoclinic
a [Å]	5.7893(1)	6.4175(1)
b [Å]	7.1947(1)	12.9740(2)
c [Å]	14.7497(2)	8.6444(1)
α [°]	88.4683(6)	90
β [°]	87.8522(5)	94.085(7)
γ [°]	68.9523(5)	90
V [Å^3]	572.909(15)	717.910(18)
T [K]	143(2)	143(2)
space group	$P\bar{1}$	$P2_1/c$
Z, D_{calc} [g cm^{-3}]	4, 1.660	4, 1.806
crystal size [mm^3]	$1.00\times0.30\times0.30$	$0.70\times0.50\times0.30$
extinction coeff.	0.093(10)	0.011(4)
μ [mm^{-1}]	0.366	0.435
$refl_{collected/unique}$	47796/3602	2258/2258
R_{int}	0.0260	–
R_1/wR_2 ($I>2\sigma(I)$)	0.0500/0.1351	0.0236/0.0635
R_1/wR_2 (all data)	0.0505/0.1356	0.0238/0.0636
$\Delta\rho_{fin}$ [e Å^{-3}]	−0.413/0.447	−0.304/0.358
CCDC no.	267373	267374

gas-phase electron diffraction apparatus.[31] The sample temperature of **3** was maintained at 258 K and that of the nozzle at 293 K to prevent sample condensation in the nozzle. Nozzle-to-camera distances of 128.05 mm and 286.11 mm were used for the short- and long-range data collections, respectively. The acceleration voltage was set to 40 kV, resulting in an electron wavelength of ≈6 pm. Precise camera distances (d) and electron wavelengths (λ) were determined by analysis of the scattering pattern of benzene immediately before or after the sample patterns were recorded. Details of the weighting functions, scattering variables, scale factors (k) and correlation parameters (q) are summarised in Table 9. The elements of the weight matrix other than diagonal and immediately off-diagonal terms were set to zero.[32] The scattering intensities were measured with an Epson Expression 1600 Pro flatbed scanner and corrected to mean optical densities as a function of the scattering variable, s, using an established program.[38] The data for the compound studied were reduced and analysed using the ed@ed[33] program with the scattering factors of Ross et al.[34]

A model of C_1 symmetry was used to describe the vapour-phase molecules of $F_3SiCH_2NMe_2$ (**3**). The structure of **3** was defined in terms of five bond lengths and differences, ten bond angles and differences, and five dihedral angles (Table 6; numbering shown in Figure 3). In accordance with the calculations, local C_{3v} symmetry was applied to describe the SiF_3 and methyl groups. An average value was employed to describe the N–C_{Me} distances, with a difference parameter to define the remaining C–N distance (p_5). Although the SiF_3 and methyl groups deviated from local C_{3v} symmetry at the highest level of calculation used, the discrepancy was small and local C_{3v} symmetry was used for these groups in the gas electron diffraction (GED) model. Within the SiF_3 group, the F-Si-F angle (p_6) was utilised to generate the C-Si-F angles. Differences in the individual C-Si-F angles were then accounted for by applying ratios of a difference parameter (p_7).

Curvilinear perpendicular distance corrections (k_{h1}) and RMS amplitudes of vibrations (u_{h1}) were obtained from the program SHRINK[35] using the force field from the B3PW91/6-311++G** calculation. The independent parameters and RMS amplitudes of vibration were then used to refine the r_{h1} structure of $F_3SiCH_2NMe_2$ in ed@ed (version 1.5) against the experimental data.

Ab initio calculations: Ab initio calculations on $F_3SiCH_2NMe_2$ were performed using the Gaussian 98 suite of programs[36] with the methods implemented therein. SCF (RHF), perturbation (MP2), and hybrid-DFT (B3LYP and B3PW91) levels of theory and Pople-type basis sets 3-21G, 6-31G and 6-311G including both diffuse and polarisation functions for heavy and light atoms were employed. Frequency calculations were performed at RHF and hybrid-DFT levels of theory to evaluate the nature of stationary points. Calculations of natural bond orbitals (NBOs) and wavefunctions, for analysis of the topology of the electron densities (using the program AIM2000),[37] were performed at the MP2/6-311G-(d,p) level. Solvent model simulations (SCIPCM), to assess the liability of the molecular geometry to change due to solvation effects, were performed using the Gaussian 03 suite of programs[36] with the methods implemented therein.

Table 9. Details of the GED experiment.

d [mm^{-1}]	Weighting functions [nm^{-1}]					q	K[a]	λ [pm^{-1}]
	Δs	s_{min}	sw_1	sw_2	s_{max}			
128.05	4.00	60	80	284	328	0.4744	0.753(20)	6.02
286.11	2.00	20	40	112	130	0.4962	0.923(17)	6.02

[a] Numbers in parentheses are estimated standard deviations of the last digit.

Acknowledgements

This work was supported by Deutsche Forschungsgemeinschaft and the Fonds der Chemischen Industrie. The authors are grateful to the Royal Society of Chemistry for a journal grant (to N.W.M.), which enabled us to meet, exchange samples and discuss the gas-phase structures and new projects, and to the EPSRC National Service for Computational Chemistry Software (administered by the Department of Chemistry, Imperial College London, South Kensington, London, SW7 2AZ) and for the computing time on Columbus.

[1] N. Egorochkin, S. E. Skobeleva, E. I. Sevast′yanova, I. G. Kosolapova, V. D. Sheludyakov, E. S. Rodionov, A. D. Kirilin, *Zh. Obshch. Khim.* **1976**, *46*, 1795.

[2] a) A. Bauer, T. Kammel, B. Pachaly, O. Schäfer, W. Schindler, V. Stanjek, J. Weis, in: *Organosilicon Chemistry V* (Eds.: N. Auner, J. Weis), p. 527, Wiley-VCH, Weinheim, **2003**; b) W. Schindler, *Adhäsion* **2004**, *12*, 29; c) *One Step Ahead—Organofunctional Silanes from Wacker*, Wacker Co., available from http://www.wacker.com/internet/webcache/de DE/BrochureOrder/GENIOSIL Brosch e.pdf.

[3] a) N. F. Lazareva, E. I. Brodskaya, G. V. Ratovsky, *J. Chem. Soc. Perkin Trans. 2* **2002**, 2083; b) N. F. Lazareva, V. P. Baryshok, M. G. Voronkov, *Russ. Chem. Bull.* **1995**, *104*, 374; c) D. Labreque, K. T. New, T. H. Chan, *Organometallics* **1994**, *13*, 332.

[4] O. Tsuge, J. Tanaka, S. Kanemasa, *Bull. Chem. Soc. Jpn.* **1985**, *58*, 1991.

[5] a) V. P. Feshin, M. G. Voronkov, *J. Mol. Struct.* **1982**, *83*, 317; b) G. Wilkinson, F. G. A. Stone, E. W. Abel, *Comprehensive Organometallic Chemistry*, *Vol. 2*, Pergamon, Oxford, **1982**, p. 412; c) R. G. Kostyanovskii, A. K. Prokof'ev, *Dokl. Akad. Nauk SSSR* **1965**, *164*, 1054; d) V. F. Mironov, A. L. Kravchenko, *Izv. Akad. Nauk SSSR Ser. Khim.* **1963**, *9*, 1563; e) M. G. Vorkonkov, V. P. Feshin, V. F. Mironov, S. A. Mikahilyants, T. K. Gar, *Zh. Obshch. Khim.* **1971**, *41*, 2211.

[6] a) D. J. Brauer, H. Bürger, S. Buchheim-Spiegel, G. Pawelke, *Eur. J. Inorg. Chem.* **1999**, 255; b) A. Ansorge, D. J. Brauer, H. Bürger, T. Hagen, G. Pawelke, *Angew. Chem. Int. Ed. Engl.* **1993**, *32*, 384.

[7] N. W. Mitzel, U. Losehand, *J. Am. Chem. Soc.* **1998**, *120*, 7320.

[8] N. W. Mitzel, U. Losehand, A. Wu, D. Cremer, D. W. H. Rankin, *J. Am. Chem. Soc.* **2000**, *122*, 4471.

[9] K. Vojinović, L. McLachlan, D. W. H. Rankin, N. W. Mitzel, *Chem. Eur. J.* ***2004***, *10*, 3033.

[10] N. W. Mitzel, C. Kiener, D. W. H. Rankin, *Organometallics* **1999**, *18*, 3437.
[11] N. W. Mitzel, *Z. Naturforsch. B*, **2003**, *58*, 369.
[12] N. W. Mitzel, *Z. Naturforsch. B*, **2003**, *58*, 759.
[13] N. Auner, R. Probst, F. Hahn, E. Herdtweck, *J. Organomet. Chem.* **1993**, *459*, 25.
[14] F. Carre, R. J. P. Corriu, A. Kpoton, M. Poirier, G. Royo, J. C. Young, C. Belin, *J. Organomet. Chem.* **1994**, *470*, 43.
[15] Yu. E. Ovchinnikov, Yu. T. Struchkov, N. F. Chernov, O. M. Trofimova, M. G. Voronkov, *J. Organomet. Chem.* **1993**, *461*, 27.
[16] V. A. Bain, R. C. G. Killean, M. Webster, *Acta Crystallogr. Sect. B* **1969**, *25*, 156.
[17] A. D. Adley, P. H. Bird, A. R. Fraser, M. Onyszchuk, *Inorg. Chem.* **1972**, *11*, 1402.
[18] C. Lustig, N. W. Mitzel, *Organometallics* **2003**, *22*, 242.
[19] R. Tacke, J. Brecht, O. Dannuppel, R. Ahlrichs, U. Schneider, W. S. Sheldrick, J. Hahn, F. Kiesgen, *Organometallics* **1996**, *15*, 2060.
[20] a) R. M. Ibberson, M. Prager, *Acta Crystallogr. Sect. B,* **1996**, *52*, 892; b) G. M. Desiraju, T. Steiner, *The Weak Hydrogen Bond*, Oxford University Press, Oxford, **1999**.
[21] J. Emsley, *The Elements*, 2nd ed., Clarendon Press, Oxford, **1991**.
[22] a) H. Jiao, P. von R. Schleyer, *J. Am. Chem. Soc.* **1994**, *116*, 7429–7430; b) K. R. Leopold, in: *Advances in Molecular Structure Research*, (Eds.: M. Hargittai, I. Hargittai), JAI Press, Greenwich, CT, **1996**, Vol. *2, p. 103*; c) K. R. Leopold, M. Canagaratna, J. A. Phillips, *Acc. Chem. Res.* **1997**, *30*, 57.
[23] C. L. Perrin, *J. Am. Chem. Soc.* **1991**, *113*, 2865.
[24] a) J. E. Carpenter, F. Weinhold, *J. Mol. Struct.* **1988**, *169*, 41; b) J. E. Carpenter, PhD thesis, University of Wisconsin, Madison, WI, **1987**; c) J. P. Foster, F. Weinhold, *J. Am. Chem. Soc.* **1980**, *102*, 7211; d) A. E. Reed, F. Weinhold, *J. Chem. Phys.* **1983**, *78*, 4066; e) A. E. Reed, F. Weinhold, *J. Chem. Phys.* **1983**, *78–79*, 1736; f) A. E. Reed, R. B. Weinstock, F. Weinhold, *J. Chem. Phys.* **1985**, *83*, 735; g) A. E. Reed, L. A. Curtiss, F. Weinhold, *Chem. Rev.* **1988**, *88*, 899; h) F. Weinhold, J. E. Carpenter, Plenum Press, **1988**, p. 227.
[25] R. F. W. Bader, *Atoms in Molecules—A Quantum Theory*, Oxford University Press, Oxford, **1990**.
[26] Important examples which show the limitations of the meaning of atomic interaction lines are: a) He@adamantane: A. Haaland, D. J. Shorokhov, N. V. Tverdova, *Chem. Eur. J.* **2004**, *10*, 4416; b) the Co–Co bond in $[Co_4(CO)_{12}]$: M. Finger, J. Reinhold, *Inorg. Chem.* **2003**, *42*, 8128; c) the bonding in solids like LiF and NaF: Y. A. Abramov, *J. Phys. Chem. A* **1997**, *101*, 5725.
[27] N. Kocher, J. Henn, B. Gostevskii, D. Kost, I. Kalikhman, B. Engels, D. Stalke, *J. Am. Chem. Soc.* **2004**, *126*, 5563.
[28] T. S. Koritsanszky, P. Coppens, *Chem. Rev.* **2001**, *101*, 1568.
[29] a) T. A. Keith, R. F. W. Bader, *J. Chem. Phys.* **1992**, *96*, 3447; b) R. S. Ruoff, T. Emilsson, A. I. jman, T. C. Germann, H. S. Gutowski, *J. Chem. Phys.* **1992**, *96*, 3441.
[30] *SHELXTL 6.10*, Bruker-AXS X-Ray Instrumentation Inc. Madison, WI, **2000**.
[31] C. M. Huntley, G. S. Laurenson, D. W. H. Rankin, *J. Chem. Soc. Dalton Trans.* **1980**, *6*, 954.
[32] Y. Murata, Y. Morino, *Acta Crystallogr.* **1966**, *20*, 605.
[33] S. L. Hinchley, H. E. Robertson, K. B. Borisenko, A. R. Turner, B. F. Johnston, D. W. H. Rankin, M. Ahmadian, J. N. Jones, A. H. Cowley, *Dalton Trans.* **2004**, 2469; http://www.ged.chem.ed.ac.uk/edated.
[34] A. W. Ross, M. Fink, R. Hilderbrandt, *International Tables for Crystallography*, *Vol. C* (Ed.: A. J. C. Wilson), Kluwer, Dordrecht, **1992**, p. 245.
[35] a) V. A. Sipachev, *J. Mol. Struct.* **1985**, *121*, 143; b) V. A. Sipachev in: *Advances in Molecular Structure Research*, *Vol. 5* (Eds.: I. Hargittai, M. Hargittai), JAI, Greenwich, **1999**, p. 263.
[36] a) Gaussian 98, revision A7, M. J. Frisch, G. W. Trucks, H. B. Schlegel, G. E. Scuseria, M. A. Robb, J. R. Cheeseman, V. G. Zakrzewski, J. A. Montgomery, R. E. Stratmann, J. C. Burant, S. Dapprich, J. M. Millam, A. D. Daniels, K. N. Kudin, M. C. Strain, O. Farkas, J. Tomasi, V. Barone, M. Cossi, R. Cammi, B. Mennucci, C. Pomelli, C. Adamo, S. Clifford, J. Ochterski, G. A. Petersson, P. Y. Ayala, Q. Cui, K. Morokuma, D. K. Malick, A. D. Rabuck, K. Raghavachari, J. B. Foresman, J. Cioslowski, J. V. Ortiz, B. B. Stefanov, G. Liu, A. Liashenko, P. Piskorz, I. Komaromi, R. Gomperts, R. L. Martin, D. J. Fox, T. Keith, M. A. Al-Laham, C. Y. Peng, A. Nanayakkara, C. Gonzalez, M. Challacombe, P. M. W. Gill, B. G. Johnson, W. Chen, M. W. Wong, J. L. Andres, M. Head-Gordon, E. S. Replogle, J. A. Pople, Gaussian Inc., Pittsburgh, PA, **1998**; b) Gaussian 03, revision C.02, M. J. Frisch, G. W. Trucks, H. B. Schlegel, G. E. Scuseria, M. A. Robb, J. R. Cheeseman, J. A. Montgomery, Jr., T. Vreven, K. N. Kudin, J. C. Burant, J. M. Millam, S. S. Iyengar, J. Tomasi, V. Barone, B. Mennucci, M. Cossi, G. Scalmani, N. Rega, G. A. Petersson, H. Nakatsuji, M. Hada, M. Ehara, K. Toyota, R. Fukuda, J. Hasegawa, M. Ishida, T. Nakajima, Y. Honda, O. Kitao, H. Nakai, M. Klene, X. Li, J. E. Knox, H. P. Hratchian, J. B. Cross, V. Bakken, C. Adamo, J. Jaramillo, R. Gomperts, R. E. Stratmann, O. Yazyev, A. J. Austin, R. Cammi, C. Pomelli, J. W. Ochterski, P. Y. Ayala, K. Morokuma, G. A. Voth, P. Salvador, J. J. Dannenberg, V. G. Zakrzewski, S. Dapprich, A. D. Daniels, M. C. Strain, O. Farkas, D. K. Malick, A. D. Rabuck, K. Raghavachari, J. B. Foresman, J. V. Ortiz, Q. Cui, A. G. Baboul, S. Clifford, J. Cioslowski, B. B. Stefanov, G. Liu, A. Liashenko, P. Piskorz, I. Komaromi, R. L. Martin, D. J. Fox, T. Keith, M. A. Al-Laham, C. Y. Peng, A. Nanayakkara, M. Challacombe, P. M. W. Gill, B. Johnson, W. Chen, M. W. Wong, C. Gonzalez, J. A. Pople, Gaussian Inc., Wallingford, CT, **2004**.
[37] a) F. Biegler-König, J. Schönbohm, D. Bayles, *J. Comput. Chem.* **2001**, *22*, 545.
[38] J. R. Lewis, R. J. Mawhorter, S. L. Hinchley, D. W. H. Rankin, unpublished results.

Received: March 29, 2005
Published online: June 30, 2005

